SAFETY ON PUNCHING OF PRESTRESSED FLAT SLABS

Ramos, A., Lúcio, V.
Department of Civil Engineering, Sciences and Technology Faculty, New University of Lisbon, UNIC-Centro de Investigação em Estruturas e Construção da UNL, Monte de Caparica, 2829-516 Caparica, Portugal

INTRODUCTION

Prestressed flat slabs have been in use for several decades now. The advantages between this structural solution and a non-prestressed flat slab are various, e.g.: smaller deformations; enables deflections and cracks under service conditions to be kept under control; allows larger spans and thinner slabs, which implies reduced costs of materials and labour; less weight also originates smaller seismic forces, which is an important factor in seismic zones.

Punching resistance is an important subject in the design of prestressed concrete flat slabs. The punching failure mechanism results from the superposition of shear and flexural stresses near the column, and is associated with the formation of a pyramidal plug of concrete which punches through the slab. It is a local and brittle failure mechanism.

Research has been developed in this subject by several authors [1-6]. The present work reports the experimental analysis of reduced scale prestressed flat slab models under punching. Fifteen models were tested, using unbonded prestress with high strength steel tendons. This work aims to improve the understanding of the behaviour of prestressed flat slabs under punching load in order to properly evaluate the safety to punching of this kind of structures.

The in-plane force effect on the punching resistance, the vertical component of the tendon forces near the column and the distance of the tendons from the column, are analysed separately.

The experimental results are compared with the recommendations of CEB-FIP Model Code 1990 [7] and the Eurocode 2- Final Draft [8]. Based on the experimental studies performed, design recommendations are also presented.

Keywords: Punching, Flat slab, Prestress, Reinforced concrete, Experimental analysis

EXPERIMENTAL MODELS

The experimental analysis described in this paper consisted in the testing of fifteen reduced scale prestressed flat slabs models up to failure by punching, divided into three sets: one for the analysis of the in-plane force effect on the punching resistance (six models), the second one to study the effect of the vertical component of the tendon forces near the column (four models), and the last one to analyse the effect of the distance of the tendons from the column on the punching resistance (five models).

The specimens were 2300x2300 mm^2 and 100 mm thick. They modelled the area near a column of an interior slab panel up to the zero moment lines. The bottom and top reinforcement consisted of 6 mm rebars every 200 mm and 10 mm rebars every 60 mm, respectively, in both orthogonal directions. The mean effective depths were 80 mm.

In the first set (models AR2 to AR7) the vertical punching load was applied by two hydraulic jacks positioned under the laboratory floor (Fig. 1). The load was transferred to the top of the slab by steel tendons and a steel frame. The slab was supported on a steel plate 200x200 mm^2, which simulated the column. In the other models (AR8 to AR16) the punching force was applied by one hydraulic jack positioned under the slab, through a steel plate with 200x200 mm^2 in the centre of the slab. The borders of the slab were connected by tendons to the strong floor of the laboratory (Fig. 5).

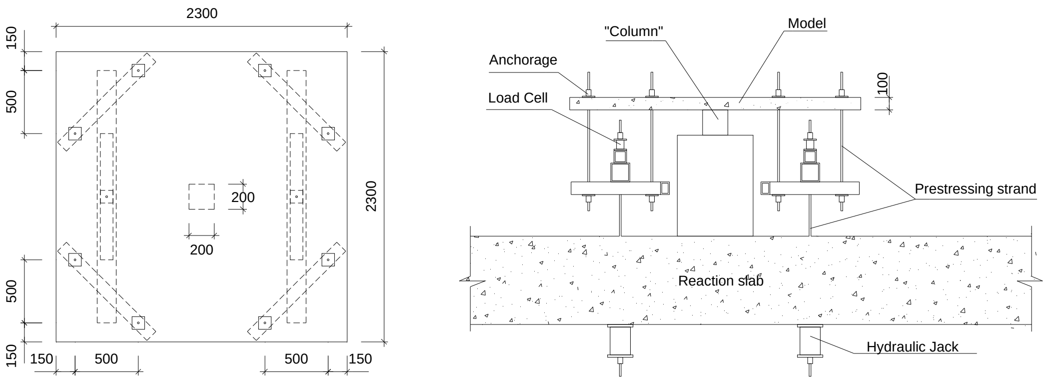

Figure 1 - Test geometry (models AR2 to AR7)

Materials Properties

To assess the strength of the concrete used in the production of the test specimens, compression tests on cubes of 15x15x15cm^3 were carried out ($f_{cm,cube}$). The results are listed in Tab. 1. This table also presents the values considered for the cylinder compression strength (f_{cm}) and for the axial tensile strength of the concrete (f_{ctm}).

Table 1 - Concrete Properties

Model	$f_{cm,cube}$ (MPa)	f_{cm} (MPa)	f_{ctm} (MPa)
AR2	48.9	39.1	3.0
AR3	46.8	37.5	2.9
AR4	53.9	43.1	3.2
AR5	44.6	35.7	2.8
AR6	46.2	37.0	2.8
AR7	54.8	43.9	3.3
AR8	52.0	41.6	3.1
AR9	46.4	37.1	2.9
AR10	51.8	41.4	3.1
AR11	47.5	38.0	2.9
AR12	39.1	31.3	2.5
AR13	40.6	32.5	2.5
AR14	35.2	28.2	2.2
AR15	39.6	31.7	2.5
AR16	38.2	30.6	2.4

The reinforcement steel tensile yielding and breaking strength used in the models is given in Tab. 2 below. The high strength steel tendons used for prestressing had a tensile 0.1 % proof strength of 1810 MPa.

Table 2 - Reinforcement Steel Properties

Models	Ø6		Ø10	
	f_{sy} (MPa)	f_{su} (MPa)	f_{sy} (MPa)	f_{su} (MPa)
AR2 to AR7	639	732	523	613
AR8 to AR13	555	670	481	633
AR14 to AR16	583	604	690	720

EFFECT OF THE IN-PLANE FORCE

Five specimens were made and tested (AR3 to AR7) with in-plane force. One specimen (AR2) was tested without prestress for comparison purpose. The in-plane forces were applied by hydraulic jacks and prestressing tendons on beams that compressed the concrete slab borders (Fig. 2). The prestress tendons were positioned outside the slab. The strains in the top reinforcement steel, the vertical displacements of the slab at nine points, the total applied load and the actual in-plane forces on the prestressing tendons, at each load stage, were measured during the tests.

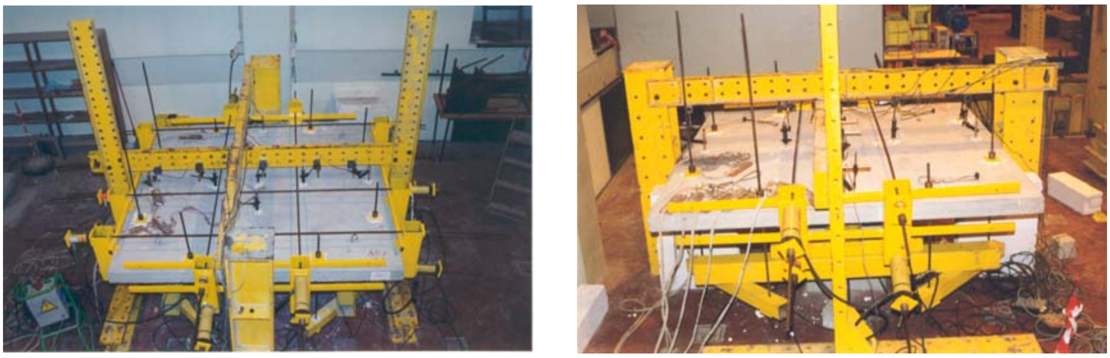

Figure 2 - System used to apply the in-plane force

Tests Results

The slab specimens were prestressed and then loaded with a vertical force until a punching failure occurred. The prestress force was kept constant during the test. The experimental results are compared with the predicted punching resistance quantified using CEB-FIP Model Code 90 – MC90 [7] and the Eurocode 2 – EC2 [8] (Tab. 3). Since the CEB-FIP Model Code 90 does not deal with prestressed slabs it was used the FIP Recommendations for the Design of Post-Tensioned Slabs and Foundation Rafts, that were published in 1998 [9, 10]. In this document both the in-plane force and the deviation force of the prestress are considered in the action side, while the punching resistance of the prestressed slab is considered as it is presented in MC90 for non prestressed slabs. In the quantification of the punching resistance the mean values of the materials strengths, without partial coefficients, were used. The limitation of the parameter ($1+\sqrt{200/d}$) in EC2 to a maximum of 2 was neglected.

Table 3 - Comparison between experimental and predicted failure loads (models AR2 to AR7)

Model	$\sigma_{cp,x}$ (MPa) (1)	$\sigma_{cp,y}$ (MPa) (1)	V_{exp} (kN) (2)	Code	V_{eff} (kN) (3)	V_{Rm} (kN) (4)	V_{eff}/V_{Rm}
AR2	0	0	258	MC90	258	270	0.96
				EC2	258	270	0,96
AR3	2.0	0	270	MC90/FIP	265	266	1.00
				EC2	270	288	0,94
AR4	3.1	0	252	MC90/FIP	244	279	0.88
				EC2	252	312	0,81
AR5	2.0	2.0	251	MC90/FIP	241	261	0.92
				EC2	251	306	0,82
AR6	1.9	2.0	250	MC90/FIP	240	265	0.91
				EC2	250	308	0,81
AR7	2.8	2.7	288	MC90/FIP	274	280	0.98
				EC2	288	340	0,85

(1) Mean compression stress due to prestress; (2) Experimental failure load; (3) Effective punching force: MC90 - $V_{eff}=V_{exp}-V_0$, EC2 - $V_{eff}=V_{exp}$, where V_0 is the decompression punching force; (4) Predicted failure load

For this set of experimental tests, the average of the ratio V_{eff}/V_{Rm} using MC 90 and the FIP recommendations was 0.94 for the prestressed models, and 0.96 for the non prestress model. Using the EC2, it was obtained an average for the same ratio of 0.85 for the five prestressed models tested. That value is against safety by a margin of approximately 15%, since the optimum value would be 1.00. It is the authors opinion that the recommended value in EC2 for the K_1 (0.10) is too high.

To better analyse the influence of the in-plane force on the punching resistance, the following graphic was made, where the experimental failure load was divided by the cubic root of the concrete compressive strength. The in-plane prestress effect, as it was modelled, seems to have little effect on the punching resistance.

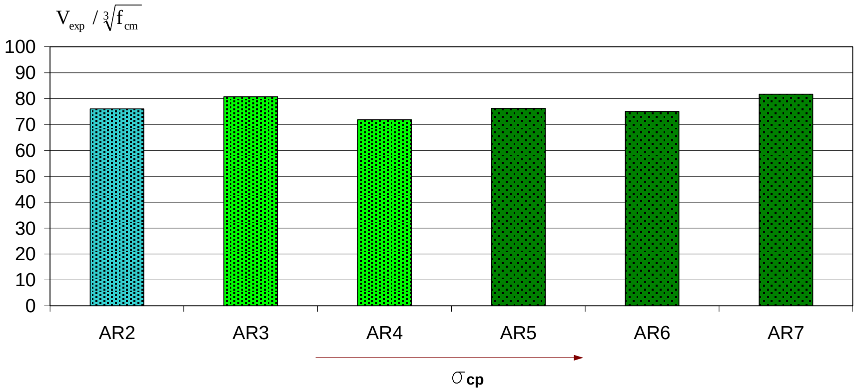

Figure 3 – Evolution of $V_{exp} / \sqrt[3]{f_{cm}}$ in Models AR2 to AR7

The presence of the in-plane compression leaded to smaller vertical deflections and smaller strains in the top reinforcement above the column. The compression force delayed the beginning of the inclined cracking across the slab thickness: that phenomenon started at about 40% of the experimental failure load in test AR2 (without compression), and 60 to 70% of the experimental failure load in the others. The angle between the punching failure surface and the horizontal varied between 30º and 35º on the specimens tested.

Figure 4 – Angle between the punching failure surface and the horizontal in Model AR2

EFFECT OF THE DEVIATION FORCE

Nine specimens of reinforced concrete slabs were made and tested up to punching failure (AR8 to AR16). All the test slabs were prestressed, except slab AR9 that was used for comparison. The prestress consisted on four unbonded 12.7 mm (0.5") diameter tendons in two orthogonal directions (Fig. 6). The nine specimens were divided into two sets: one with all the tendons crossing the loaded area (Models AR8, AR10 and AR11) and another with the tendons placed at different distances from the loaded area (Models AR12 to AR16).

The strains in the top reinforcement steel, the vertical displacements of the slab at nine points, the total applied load and the actual prestress force on the tendons were measured during the tests.

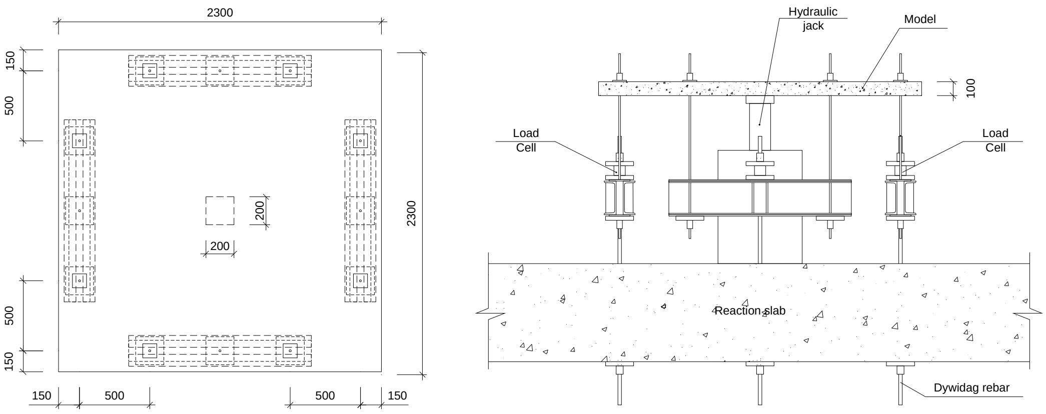

Figure 5 - Test geometry (models AR8 to AR16)

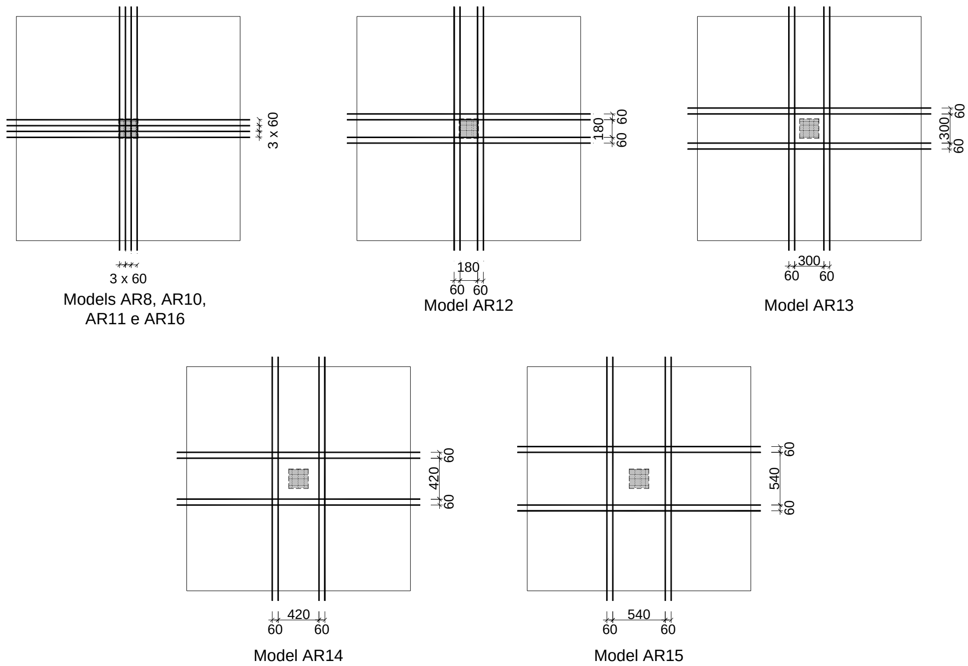

Figure 6 – Prestressed tendons location

The tendons profiles were trapezoidal, with the downward tendon deviation forces over the loaded area and the upward deviation forces at 1000 mm from the centre of the loaded area.

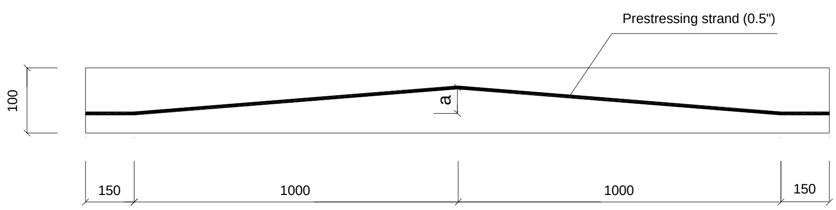

Figure 7 – Tendon trapezoidal shape

Table 4 – Prestress vertical deviation (measured during constrution of the models)

Modelo	AR8	AR10	AR11	AR12	AR13	AR14	AR15	AR16
a_x(mm)	39.3	40.3	42.2	36.9	39.9	32.4	34.3	42.4
a_y(mm)	41.3	40.7	41.6	36.6	36.7	37.9	39.4	40.5

The prestress forces were applied to the tendons by eight (four in each direction) hydraulic jacks. The intention of these tests was to study only the effect of the vertical deviation forces of the prestressing tendons. Steel frames were used to avoid the compression force of the prestress to be transmitted to the slab (Fig. 8). With the slab deformation the tendons have the tendency to increase their prestress force, especially if they are short ones. A load maintainer device was used in these hydraulic jacks in order to keep the prestress force constant during the tests.

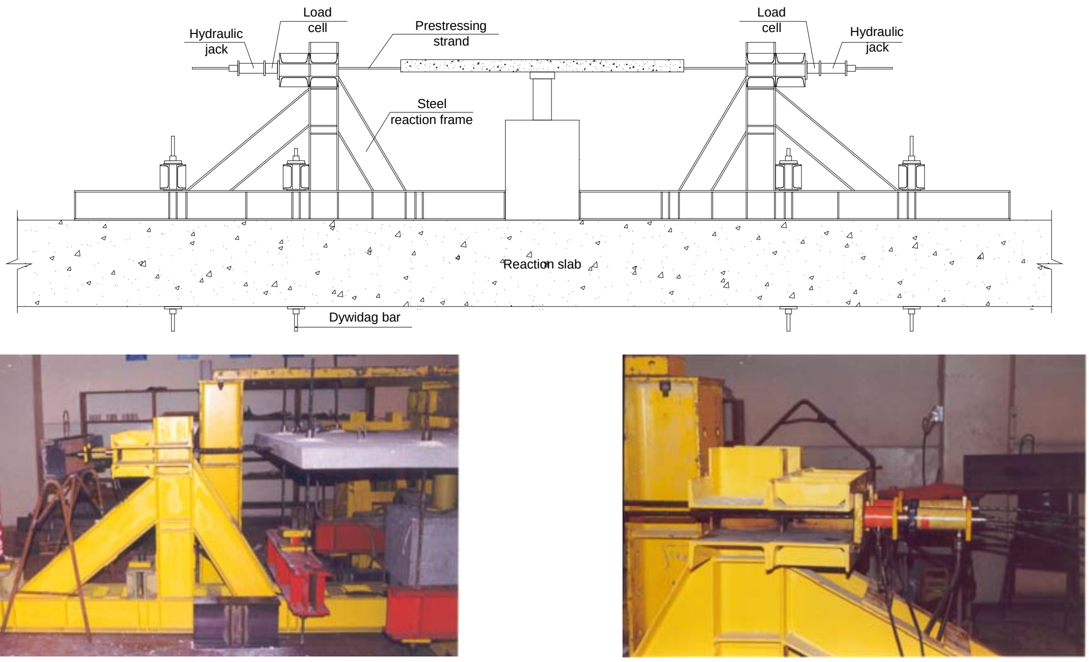

Figure 8 – Steel reaction frame

Tests Results

The models were loaded with an initial 50 kN vertical load, and afterwards the prestress was applied. Then the vertical load was increment until a punching failure occurred. The experimental results are compared with the predicted punching resistance quantified using CEB-FIP Model Code 90 – MC90 [7] and the Eurocode 2 – EC2 [8] (Tab. 5). In this particular case the two codes are virtually the same, with only a slight difference: the FIP Recommendations for the Design of Post-Tensioned Slabs and Foundation Rafts recommends that the vertical component of the tendon force to be included in the punching calculation takes only into account the prestressing tendons passing within a distance of 0.5h of the loaded area, were h is the thickness of the slab, and EC2 considers 0.5d, were d is the effective depth of the slab.
The EC2 has some contradictory information regarding that last statement. In fact, in 6.4.3 (9) it recommends that the vertical component resulting from inclined prestressing tendons crossing the control section (2.0d) may be taken into account as favourable, and in 9.4.3 it states that the vertical component of only those prestressing tendons passing within a distance of 0.5d of the column may be included in the shear calculation. In the authors opinion, based on the experimental analysis carried out, the last recommendation should be adopted. The present research also proves that considering the tendons positioned at more than 0.5d from the loaded area in that calculation is against safety.

Figure 9 – Tendon location and punching shear failure surface

Table 5 - Comparison between experimental and predicted failure loads (models AR8 to AR12)

Model	P (kN) (1)	a (mm)	V_{exp} (kN) (2)	V_{dev} (kN) (3)	V_{eff} (kN) (4)	V_{Rm} (kN) (5)	V_{eff}/V_{Rm}
AR9	-	-	251	-	251	273	0.92
AR8	448	40.3	380	72	308	278	1.11
AR10	348	40.5	371	56	315	278	1.13
AR11	239	41.9	342	40	302	269	1.12
AR12	448	36.8	280	66	214	239	0.90
AR13	446	38.3	261	34	227	253	0.90
AR14	431	35.2	208	0	208	240	0.87
AR15	445	36.9	262	0	262	250	1.05
AR16	442	41.5	351	74	277	249	1.11

(1) Prestress force in each orthogonal direction; (2) Experimental failure load; (3) Vertical component of the prestress force (deviation force); (4) Effective failure load: $V_{eff}=V_{exp}-V_{dev}$; (5) Predicted failure load (MC90 or EC2)

The average of the ratio V_{eff}/V_{Rm} using either MC 90 or EC2 for the group of models where the tendons crossed the loaded area (Models AR8, AR10, AR11 and AR16) was 1.12. This result is conservative, probably because the initial vertical deviation of the tendons was used in the calculation of the deviation force. In fact, as the slab deforms during loading, the vertical deviation of the tendons increases, and consequently the same happens to the prestress deviation force.

If only the prestressing tendons passing within a distance of 0.5d of the loaded area are used in the calculation of the deviation force, the average of the ratio V_{eff}/V_{Rm} for models AR12 to AR15 is 0.93. For the model without prestress (AR9) this ratio was 0.92.

To better understand the influence of the deviation force on the punching resistance the following graphics were made, where the experimental failure load was divided by the cubic root of the concrete compressive strength (Fig. 10 and 11), in order to make it independent of the concrete quality.

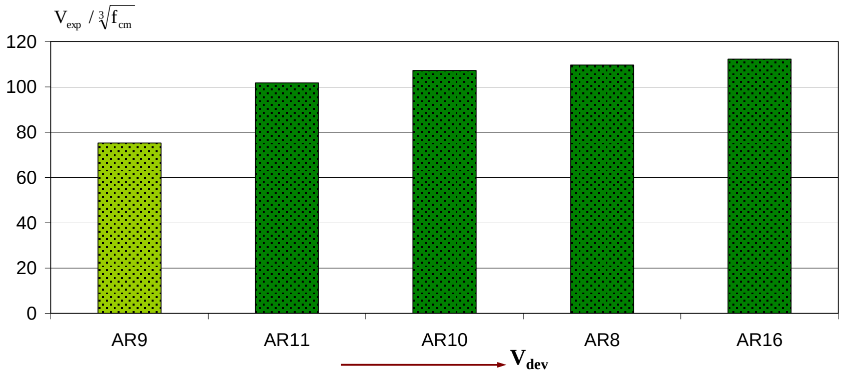

Figure 10 – Evolution of $V_{exp} / \sqrt[3]{f_{cm}}$ in Models AR8 to AR11 and AR16

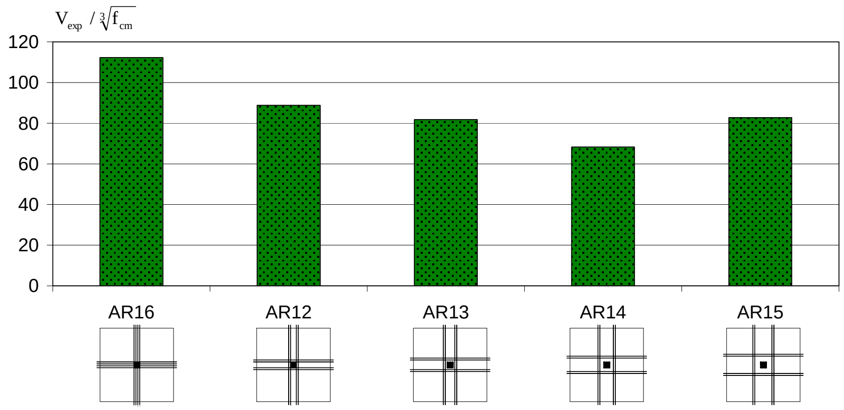

Figure 11 – Evolution of $V_{exp} / \sqrt[3]{f_{cm}}$ in Models AR12 to AR16

The increasing of the prestress force, and consequently the increasing of the deviation force, leaded to an increment on the punching resistance. Increasing the distance between the tendons and the column resulted, in general, in lower punching resistances.
The strains in the top reinforcement on the prestressed models were smaller than in model AR9 (without prestress). Increasing the distance between the tendons and the column caused a small increment in the top reinforcement strains.
The presence of prestress force delayed the beginning of the inclined cracking across the slab thickness. That phenomenon started at about 120 kN for Model AR9, 150 kN for Model AR11, 180 kN for Model AR10 and 200 kN for Model AR8. The angle between the punching failure surface and the horizontal varied between 29º and 36º on the specimens tested.

CONCLUSIONS

Three sets of tests of prestressed flat slabs under punching were performed. In the first set, only in-plane prestress was applied with external tendons (test slabs AR3 to AR7). In the second and third sets, internal tendons were used with a trapezoidal shape to impose deviation forces on the slab (test slabs AR8 and AR10 to AR16). In the last two sets of tests, no compression due to prestress was applied to the slab. It was possible to analyse separately the two prestress effects in this study. The test results were compared with the predicted values of the MC90 and EC2. Two non-prestressed slabs were also tested (AR2 and AR9) in order to compare the results.
The in-plane compression due to the prestress seems to have little effect on the punching resistance of the tested specimens.
On the other hand, the presence of the deviation force above the loaded area, resulting from inclined prestressing tendons, leaded to an increment on the punching resistance. The opposite happened with the increase of the distance between the tendons and the column. In the estimation of the deviation force only the tendons that are at less than d/2 from the column perimeter should be considered.
In general, the prestress presence delayed the beginning of the inclined cracking across the slab thickness that origin the punching failure, resulted in smaller strains in the top reinforcement and smaller vertical deflections of the slabs tested.

REFERENCES

1. Scordelis, A. C., Lin, T.Y. and May, H. R., “Shearing strength of prestressed lift slabs”, ACI Journal, October, 1958, pp 485-506.
2. Nylander, H.; Kinnunen, S.; Ingvarsson, H.: Genomsstansning av Pelarunderstödda Plattbro av Betong med Spänd och Ospänd Armering, Meddelande nº 123, KTH, Stockholm, 1977.
3. Pralong, J.; Brändli, W.; Thürlimann, B.: Durchstanzversuche an Stahlbeton und Spannbetonplatten, Bericht nr. 7305-3, Institut für Baustatik und Konstruktion, ETH Zurich, December, 1979.
4. Shehata, I. A., “Punching of prestressed and non-prestressed reinforced concrete flat slabs”, M Phil Thesis, Polytechnic of Central London, Sept, 1982.
5. Regan, P. E., “Punching shear in prestressed concrete slab bridges”, Structures Research Group, Polytechnic of Central London, Jan, 1983.
6. Hassanzadeh, G.; Sundquist, H.: Influence of Post-Tensioned Reinforcement Distribution on Design of Prestressed Reinforcement in Column Supported Flat Slabs, Proceedings of the International Workshop on Punching Shear Capacity of RC Slabs, Stockholm, June, 2000, p.457-466.
7. Comité Euro-International du Betón: CEB-FIP Model Code 1990, Bulletin d´information nº 213-214, May, 1993.
8. Eurocode 2 : Design of concrete structures – Part 1-1: General rules and rules for buildings, December 2004.
9. Fédération Internationale de la Précontrainte: “Recommendations for the Design of Post-Tensioned Slabs and Foundation Rafts”, May, 1998.
10. Lúcio, V. J. G.; Appleton, J. A. S.; Almeida, J. F.: The U.L.S. of Punching in the New FIP Recommendations for the Design of Post-Tensioned Slabs and Foundation Rafts, Structural Concrete - FIP, nº 3, 2000.